Effects of Mechanical Strains on the Characteristics of Top-Gate Staggered a-IGZO Thin-Film Transistors Fabricated on Polyimide-Based Nanocomposite Substrates

Chang-Yu Lin, Chih-Wei Chien, Chung-Chih Wu, Yung-Hui Yeh, Chun-Cheng Cheng, Chih-Ming Lai, Ming-Jiue Yu, Chyi-Ming Leu, and Tzong-Ming Lee

***Abstract*—In this paper, we had successfully implemented flexible top-gate staggered amorphous In–Ga–Zn–O (a-IGZO) thin-film transistors (TFTs) on colorless and transparent polyimide (PI)-based nanocomposite substrates using fully lithographic and etching processes that are compatible with existing TFT mass fabrication technologies. The use of the selectively coated release layer between the nanocomposite PI film and the glass carrier ensured smooth debonding of the plastic substrate after TFT fabrication. The TFTs showed decent performances (with mobility $> 10\ \mathrm{cm^2/V \cdot s}$) either as fabricated or as debonded from the carrier glass. By bending the devices to different radii of curvature (from a flat state to an outward bending radius of 5 mm), influences of mechanical strains on the characteristics of flexible a-IGZO TFTs were also investigated. In general, the mobility of the flexible a-IGZO TFT increased with the tensile strain, whereas the threshold voltage decreased with the tensile strain. The variation of the mobility in a-IGZO TFTs versus the strain appeared smaller than those observed for amorphous silicon TFTs.**

***Index Terms*—In–Ga–Zn–O, mechanical strain, nanocomposite, polyimide (PI), thin-film transistors (TFTs).**

I. Introduction

IN RECENT YEARS, flexible electronics and displays have attracted much attention due to their various merits such as light weight, thin profiles, portability, and their abilities to form conformable shapes, giving various possible novel applications [1]–[3]. Suitable active materials and flexible substrates are key components to realize flexible electronics and displays. Amorphous silicon (a-Si:H) and organic semiconductors are two common candidates for the active materials of flexible thin-film transistors (TFTs) [4]–[6]. However, these materials usually have limited performances such as low mobility around or below $\sim 1\ \mathrm{cm^2/V \cdot s}$. On the other hand, the TFT technology based on oxide semiconductors, particularly amorphous In–Ga–Zn–O (a-IGZO), is emerging as a promising option for flexible electronics due to their various merits such as high mobility in the amorphous phase, low processing temperatures, and relative compatibility with the existing TFT fabrication technologies [7], [8]. As for flexible substrates, in general, three types of substrates are available for flexible electronics, namely, metal foils, thin flexible glasses, and plastic substrates [3], [9], [10]. In these materials, flexible glasses are fragile and difficult to handle, and metal foils suffer limited flexibility/rollability and issues of parasitic capacitance. Plastic substrates are highly flexible, unbreakable, lightweight, and suitable for roll-to-roll processing, ideal for flexible electronics. However, the thermal and dimensional stability are important concerns for plastic substrates [11]. As such, plastic substrates based on polyimides (PIs) that can stand higher processing temperatures have been recognized as one important class of flexible plastic substrates [12]–[14], although nowadays, most available PIs to date are colored or not transparent, limiting possible applications in flexible electronics, particularly in displays.

In this paper, we report fabrication of flexible a-IGZO TFTs on transparent and flexible PI-based nanocomposite substrates using fully lithographic, etching, and plasma-enhanced chemical vapor deposition (PECVD) processes that are compatible with existing TFT mass production technologies. We also conducted studies of influences of mechanical strains on flexible a-IGZO TFTs. Although there had been some previous reports of flexible oxide TFTs or a-IGZO TFTs on plastic substrates and even their applications (e.g., flexible displays) [12]–[18], in general, the fabrication of micrometer-scale/miniaturized oxide TFTs on plastic substrates is still not trivial. In addition, to meet the stringent requirements in either applications or manufacturing of flexible electronics, more understanding of effects of mechanical strains on flexible oxide TFTs is still required.

Manuscript received November 7, 2011; revised February 25, 2012; accepted March 29, 2012. Date of publication May 4, 2012; current version published June 15, 2012. This work was supported in part by the Ministry of Economic Affairs, by the Electronics and Optoelectronics Research Laboratories of the Industrial Technology Research Institute, by the National Science Council of Taiwan, and by the Ministry of Education of Taiwan under Grant 10R70607-2. The review of this paper was arranged by Editor H.-S. Tae.

C.-Y. Lin is with the Graduate Institute of Photonics and Optoelectronics, National Taiwan University, Taipei 106, Taiwan.

C.-W. Chien and C.-C. Wu are with the Department of Electrical Engineering, the Graduate Institute of Electronics Engineering, and the Graduate Institute of Photonics and Optoelectronics, National Taiwan University, Taipei 106, Taiwan (e-mail: chungwu@ cc.ee.ntu.edu.tw).

Y.-H. Yeh, C.-C. Cheng, C.-M. Lai, C.-M. Leu, and T.-M. Lee are with the Industrial Technology Research Institute, Hsinchu 310, Taiwan.

M.-J. Yu is with National Chiao Tung University, Hsinchu 300, Taiwan, and also with the Industrial Technology Research Institute, Hsinchu 310, Taiwan.

Digital Object Identifier 10.1109/TED.2012.2193585

0018-9383/$31.00 © 2012 IEEE

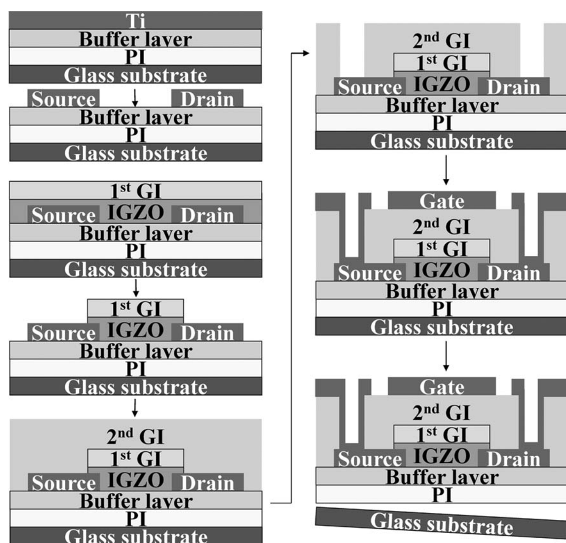

Fig. 1. Device structure and microfabrication processes for the top-gate staggered a-IGZO TFTs on a PI/glass carrier.

II. EXPERIMENTS

A. Fabrication of TFTs on PI-Based Nanocomposite Substrates Using Glass Carriers

Although oxide TFTs could be possibly fabricated at room temperature, it has been shown, however, that a higher processing temperature (e.g., postannealing above 200 °C) would improve device performance, e.g., stability [19]–[21]. Thus, a PI that can stand high processing temperatures is one preferable candidate plastic substrate for fabricating flexible oxide TFTs. However, most available high-temperature PIs are usually colored, not fully transparent. In this paper, we adopted the high-temperature and transparent/colorless PI-based nanocomposite substrates developed by the Industrial Technology Research Institute (of Taiwan) [22]. These substrate materials are based on the hybrid organic/inorganic nanocomposites of PI and nanosilica (with high silica contents of $\geq$50 wt.%), which allow wide tuning of the thermal, optical, and coating properties and yield PI-based nanocomposites featuring high glass-transition temperature ($Tg > 300$ °C), high transmittance in the visible range ($\sim$90%), and reduced coefficients of thermal expansion (CTEs, < 30 ppm/°C) [22], [23]. In using these substrate materials for TFT fabrication, glass substrates were used as the carrier substrates, on which smooth PI-based nanocomposite films (with a thickness of tens of micrometers) can be nicely coated with convenient coating techniques such as slot coating and blade coating.

Fig. 1 shows the device structure and the microfabrication processes for the top-gate staggered a-IGZO TFTs on a PI/glass carrier using the 4-mask lithography/etching process and a maximum processing temperature of ≤ 210 °C. First, the SiN_x buffer layer was deposited on the PI substrate by PECVD to serve as the moisture barrier and to withstand the chemicals used in TFT processing. Then, 30-nm-thick Ti was deposited by sputtering, followed by lithography and wet etching to define the source/drain electrodes. Next, 40-nm-thick a-IGZO was deposited by RF sputtering using the 6-in $In_2Ga_2ZnO_7$ target (purchased from LTS Chemical, Inc.), a working pressure of 1 mtorr, an RF power value of 300 W, and no intentional heating of the substrate. The O_2 to $(Ar + O_2)$ gas-flow ratio of 1/5 $[O_2 : (Ar + O_2) = 10{:}50$ SCCM$]$ was used for deposition of the a-IGZO channel layer. Subsequently, a first gate insulator (first GI) of 50-nm-thick SiO_x was deposited by PECVD at 200 °C. The first gate insulator layer was used as the protection layer for a-IGZO, the hard mask for a-IGZO etching, and also as a part of the gate insulator. The deposition conditions of PECVD SiO_x included 5% N_2 diluted SiH_4 gas-flow rate of 160 SCCM, N_2O gas-flow rate of 710 SCCM, a chamber pressure of 0.9 torr, and an RF power value of 20 W. The first gate insulator was then patterned using reactive-ion etching (RIE), and then a-IGZO was patterned by weak acid using this patterned first gate insulator as the hard mask. Afterward, a second gate insulator (second GI) of 300-nm-thick SiN_x was deposited again by PECVD at 200 °C to complete the bilayer gate insulator stack. The deposition conditions of PECVD SiN_x included 5% N_2 diluted SiH_4 gas-flow rate of 250 SCCM, NH_3 gas-flow rate of 5 SCCM, N_2 gas-flow rate of 180 SCCM, a chamber pressure of 1.2 torr, and an RF power value of 25 W. The second gate insulator (SiN_x) was etched to expose the source and drain contact holes by RIE. Finally, 100-nm-thick Ti was deposited by sputtering and patterned as the gate electrode. After the device fabrication, postannealing was performed at 210 °C in air. The channel width and channel length of the TFTs were 24 and 16 μm, respectively.

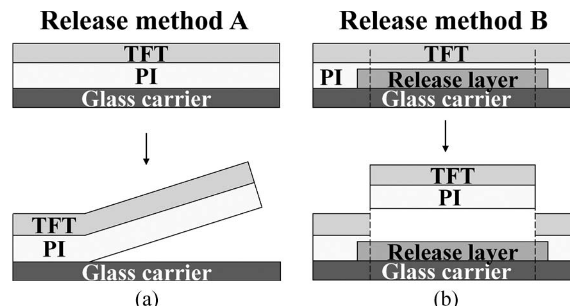

Fig. 2. (a) Illustration of the release method A. (b) Illustration of the release method B.

B. Releasing of PI-Based Nanocomposite Substrates from Glass Carriers

After the TFT fabrication on the PI/glass carrier, the PI films with completed TFTs need to be released from the glass carrier to yield the free-standing flexible TFTs. Indeed, how to release the plastic substrates from glass carriers after TFT fabrication is a critical technology for manufacturing flexible TFTs on plastic substrates with carriers. Two releasing methods, namely, methods A and B, were tested in this paper. Fig. 2(a) illustrates the release method A. In this method, the PI-based nanocomposite films were directly coated onto the glass carrier substrates. After the TFT fabrication, the PI films with completed TFTs were peeled off directly from the glass carriers. Fig. 2(b) illustrates the release method B. In this method, to permit easier separation of the flexible substrate from the carrier glass after TFT fabrication, the glass surface was selectively coated with a

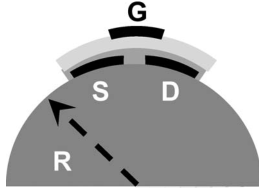

Fig. 3. Configuration for measuring the electrical characteristics of flexible a-IGZO TFTs bent to a specific radius of curvature R.

release layer (before coating of the PI-based nanocomposite) [22] to which the nanocomposite material exhibits weaker adhesion. The release layer typically used the parylene polymer that was deposited by simple thermal CVD (i.e., via pyrolysis and room-temperature polymerization/deposition of parent dimer molecules) [22]. It is a material already widely used in many large-area applications and can be coated with various convenient large-area deposition techniques, including roll-to-roll processes, having no limit in sizes. The nanocomposite film could be easily lifted after device processing by simply cutting around edges of the release-layer region [as shown in Fig. 2(b)], given free-standing flexible films. Such handling technique of plastic substrates does not require use of glue, given fewer issues of glue residues and glue-related problems [22]. Furthermore, with such techniques, TFT devices can be conveniently processed using the mature and existing TFT batch processes.

C. Characterization of Flexible a-IGZO TFTs

To study the effects of mechanical strains on a-IGZO TFTs, strain was applied onto flexible a-IGZO TFTs on PI-based nanocomposites by bending the device outward onto cylinders of varied radius of curvature R, as shown in Fig. 3. Fig. 3 shows the configuration for measuring the electrical characteristics of flexible a-IGZO TFTs bent to a specific radius of curvature R. The bending direction was parallel to the drain-to-source current path (i.e., uniaxial bending). Characterization started with bending the device to a maximum R for some extended time (to make sure the applied strain reached the stable state) and then measuring the electrical characteristics of the TFT under the bending state. This test cycle was repeated by decreasing R down to the minimum R. Under each mechanical bending state (i.e., at different R), characteristics of TFTs were measured.

The output and transfer characteristics of the top-gate a-IGZO TFTs were measured using an Agilent 4156C semiconductor parameter analyzer. The linear mobility was extracted from the linear-regime transconductance g_m at the low drain-to-source voltage ($V_{\rm DS} = 1$ V) by [24]

$$\mu_{\rm lin} = \frac{Lg_m}{WC_iV_{\rm DS}}$$

where C_i denotes the capacitance of the gate insulator per unit area, and L and W are the channel length and the channel width, respectively. g_m is the transconductance defined by

$$g_m = \left.\frac{\partial I_{rmD}}{\partial V_{\rm GS}}\right|_{V_{\rm DS}=1{\rm V}}$$

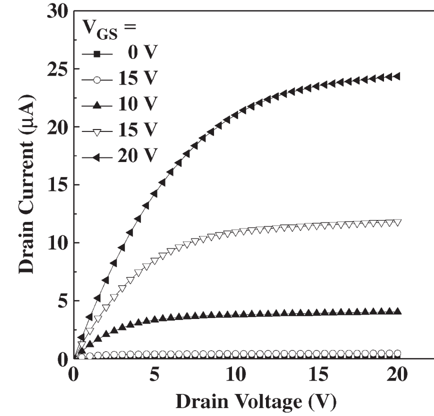

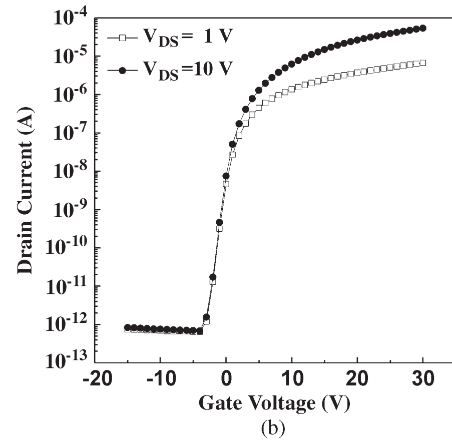

Fig. 4. (a) Output and (b) transfer characteristics of the as-fabricated a-IGZO TFT measured when the PI-based nanocomposite was still bonded on the glass carrier.

where I_{rmD} and $V_{\rm GS}$ denote the drain current and the gate voltage, respectively. The subthreshold swing (SS) was extracted from the slope of transfer characteristics (at $V_{\rm DS} = 10$ V) in the subthreshold regime

$$\mathrm{SS} = \left(\frac{\partial \log I_{rmD}}{\partial V_{\rm GS}}\right)^{-1}.$$

Threshold voltage $V_{\rm th}$ was determined by plotting $I_{rmD}^{1/2}$ versus $V_{\rm GS}$ and extrapolating the curve to zero drain current [25]. The on/off ratio was estimated from the transfer characteristics at $V_{\rm DS} = 10$ V by calculating the ratio between the maximal on current (at $V_{\rm GS} = 30$ V) and the minimal off current.

III. Results and Discussions

A. Influences of Releasing Methods on Flexible a-IGZO TFTs

Top-gate staggered a-IGZO TFTs had been successfully fabricated on the PI-based nanocomposites/glass carriers with decent performance by fully lithographic and etching processes that are compatible with existing TFT fabrication technologies. Fig. 4(a) and (b) shows the output and transfer characteristics of the as-fabricated a-IGZO TFT, which were measured when the PI-based nanocomposite was still bonded on the glass carrier. The data shown in Fig. 4 are for the nanocomposite with a release layer, but those for the nanocomposite without

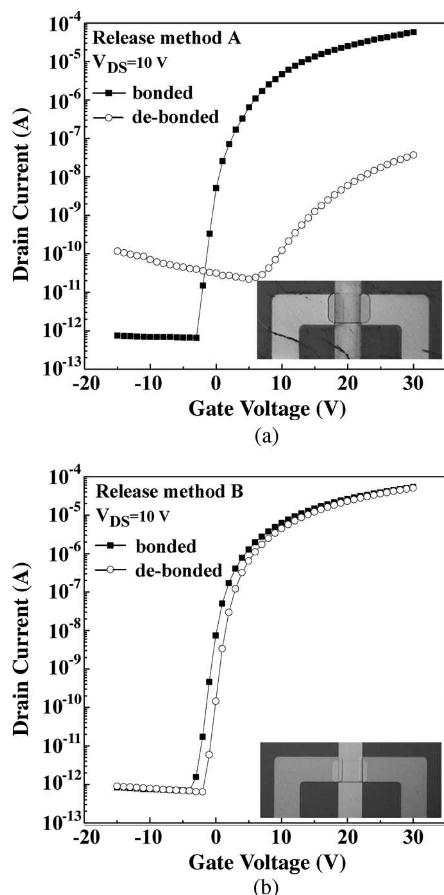

Fig. 5. (a) Transfer characteristics of the a-IGZO TFT while still bonded on the glass carrier and after being debonded from the glass carrier by the release method A. (b) Transfer characteristics of the a-IGZO TFT while still bonded on the glass carrier and after being debonded from the glass carrier by the release method B. (Insets) Photo of a-IGZO TFTs on PI debonded from the glass carrier.

the release layer are similar. The extracted linear mobility, threshold voltage, SS, and on/off ratio were 10.9 $cm^2/V \cdot s$, 0.9 V, 0.75 V/dec., and 7×10^7, respectively.

The PI-based nanocomposites were then separated from the glass carriers by the release method A (direct peeling) or the release method B (using a release layer), and then, the characteristics of flexible TFTs obtained by these two different methods were compared with those of as-fabricated TFTs (still on glass carriers). Fig. 5(a) shows the transfer characteristics of the TFT while still bonded on the glass carrier and after being debonded from the glass carrier by the release method A. After debonding, the devices were measured at the flat state and significant degradation of device characteristics was observed. After debonding, the mobility, SS, and on/off ratio degraded from 10.1 to 0.01 $cm^2/V \cdot s$, 0.7 to 4.13 V/dec., and 8×10^7 to 2×10^3, respectively. Due to rather strong adhesion between the PI-based nanocomposite and the glass, an extra external force was required to peel the PI films from the glass substrates, which could easily lead to significant deformation or cracking of completed TFTs, as shown in inset in Fig. 5.

Fig. 5(b) shows the transfer characteristics of the TFT while still bonded on the glass carrier and after being debonded from the glass carrier by the release method B. In sharp contrast

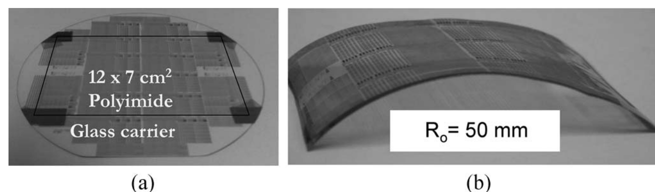

Fig. 6. (a) Photo of a 12×7 cm^2 nanocomposite PI on the glass carrier with completed a-IGZO TFTs. (b) Photo of the free-standing nanocomposite PI with completed TFTs, which was obtained by the release method B.

with TFTs separated by the release method A, the flexible TFTs obtained by the release method B still mostly retained performances of the as-fabricated TFTs, except for a slight shift of V_{th} toward the more positive voltage (from 0.9 to 1.86 V), which was due to the built-in mechanical strain remained in the structure (after all the TFT fabrication and separation steps, as will be described below). After debonding by the release method B, the mobility, SS, and on/off ratio only slight changed from 10.9 to 10.21 $cm^2/V \cdot s$, 0.75 to 0.72 V/dec., and 7×10^7 to 7×10^7, respectively. These slight changes in TFT characteristics are mainly associated with residual built-in mechanical strains remained in the structure after all the TFT fabrication and separation steps to be described below. Overall, these results indicate that with the release layer, the release method B largely reduces the impact of external forces on the PI films (as in the release method A). The performances of a-IGZO TFTs on PI films thus can be well retained.

Fig. 6(a) shows the photo of the 12×7 cm^2 nanocomposite PI on the glass carrier with completed a-IGZO TFTs. Fig. 6(b) shows the photo of the free-standing nanocomposite PI with completed TFTs, which was obtained by the release method B. The debonded PI with TFTs was naturally curved, with a natural radius of curvature $R_o = 50$ mm (i.e., the initial radius of curvature without applying any external bending force), implying that some internal built-in mechanical strain remained in the structure after all the TFT fabrication and separation steps. The built-in mechanical strains are associated with the mismatch of CTE between the glass substrate, the PI film, and TFT layers during growth of TFT layers at elevated temperatures. The CTEs of the TFT layers (e.g., PECVD SiO_x and SiN_x) and the glass carrier are typically smaller than that of the PI film [22], [26], [27].

Although the release method B largely reduces the impact of external forces on the substrates and devices (as in the release method A), there are still slight changes in TFT characteristics. These slight changes in TFT characteristics are discussed as follows. Fig. 7 illustrates how the difference in thermal expansion properties of materials would result in the built-in mechanical strains in the final free-standing PI film with TFTs. For simplicity, the release layer (polymer parylene) is not explicitly shown in Fig. 7 since it is a polymer and its thermal expansion properties are similar to those of PI. Fig. 7(a) schematically shows the initial dimensions of the glass and the nanocomposite PI film at room temperature. Fig. 7(b) schematically illustrates how the glass carrier, the nanocomposite PI film, and the TFT layers would expand when heated to 200 °C for material layer growth (e.g., TFT layers by PECVD) if all material layers were not constrained by substrates or neighboring layers. As shown

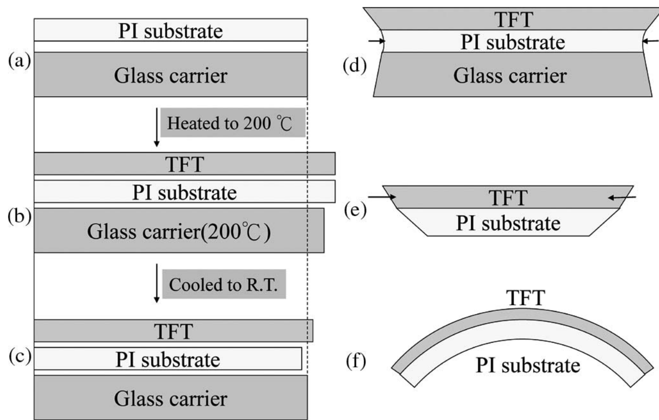

Fig. 7. Illustration of how the difference in thermal expansion properties of materials would result in the built-in mechanical strains in the final free-standing PI film with TFTs.

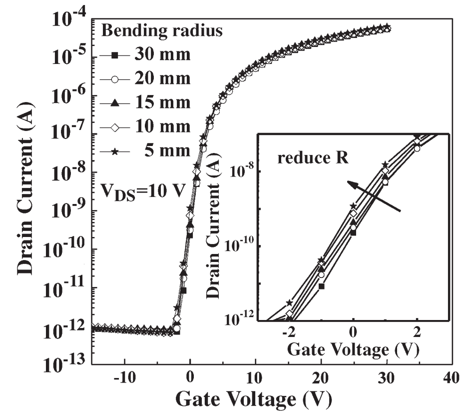

Fig. 8. Transfer characteristics of the flexible a-IGZO TFTs under different bending radii. (Inset) Enlargement of a portion of Fig. 8.

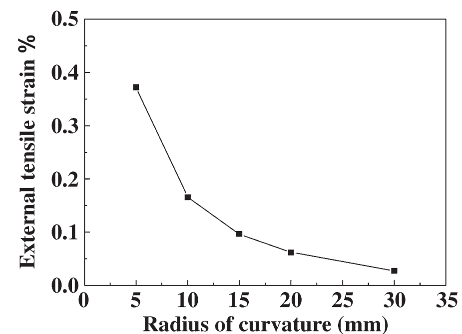

Fig. 9. Calculated external strain versus the bending radius of the nanocomposite PI with a-IGZO TFTs.

in Fig. 7(c), if all the material layers were not constrained, when cooled down to room temperature, the PI film would shrink more than the glass carrier and TFT layers since polymer films would generally shrink by heating and cooling cycles [11] and both the glass and TFT layers have smaller CTEs than PI. In considering that all the materials are actually constrained by the substrate and neighboring layers and are not freely scalable in dimensions, as illustrated in Fig. 7(d), cooling to room temperature indeed would induce compressive strains to both the glass carrier and the TFT layers. When debonded from the glass carrier [see Fig. 7(e)], without the constraint from the glass carrier, the bottom side of PI would tend to shrink more (than the top side), leading to even larger compressive strains in TFTs in the debonded sample (in the flat state) than in the bonded sample. As aforementioned, the slight change of TFT characteristics after debonding by the release method B [see Fig. 5(b)] is associated with this increase in compressive strains. If the external force holding the debonded sample flat was removed, the debonded sample would naturally exhibit a curved shape [see Fig. 7(f)].

B. Characteristics of Flexible a-IGZO TFTs Under Varied Uniaxial Strains

To further investigate the effects of mechanical strains on the characteristics of flexible a-IGZO TFTs, TFTs' characteristics were repeatedly measured when bending the device outward onto cylinders of varied radius of curvature R (see Fig. 3). Fig. 8 shows the transfer characteristics of the flexible a-IGZO TFTs under different bending radii. The inset in Fig. 8 shows the enlarged transfer curves for a smaller gate-voltage/drain-current region, which more clearly manifests the shift of the transfer characteristics of the flexible a-IGZO TFTs toward the more negative voltage when reducing the bending radius (i.e., increasing the tensile strain in TFTs, as will be explained below).

The external tensile strain applied corresponding each outward bending radius could be calculated by the strain theory and the initial strain remained in the sample after the fabrication of the flexible TFT [5]. Fig. 9 shows the calculated external strain applied versus the bending radius of the nanocomposite PI with a-IGZO TFTs. The natural radius of curvature of the PI film with completed TFTs is $R_o = 50$ mm (with initial strain of 0%). In the flat state (i.e., with $R = \infty$), it corresponds to an external compressive strain of -0.004%. The radii of the cylinders used in the bending experiment ranged from 30 to 5 mm, corresponding to the external uniaxial tensile strain of 0.03%–0.37% applied onto TFTs.

The linear mobility and threshold voltage extracted from the transfer characteristics of the flexible a-IGZO TFTs under different strains (i.e., under different bending radii) are shown in Fig. 10(a) and (b), respectively, as a function of the mechanical strains. As shown in Fig. 10(a), in applying the uniaxial strain of -0.004%–0.37% (i.e., the bending radius R from ∞ (flat state) to 5 mm) to the flexible a-IGZO TFTs, the linear mobility varied from 10.21 to 10.67 $\mathrm{cm^2/V \cdot s}$. Meanwhile, Fig. 10(b) shows that in applying the uniaxial strain of -0.004%–0.37% to the flexible a-IGZO TFTs, the threshold voltage varied from 1.86 to 1.57 V. The dependence of the mobility and threshold voltage on the strain appears to be nonlinear (e.g., stronger dependence at the strain $< 0.1\%$ and weaker dependence at the strain $> 0.1\%$). It is interesting to note that, regardless if strain is larger or smaller than 0.1%, the slope of strain-induced mobility variation for a-IGZO TFTs is significantly lower than those observed for a-Si TFTs [6]. Such a result suggests that a-IGZO (formed by ionic bonding) might potentially have better flexibility than a-Si (formed by covalent bonding).

The tensile strain, in general, increases the interatomic distance in the semiconductor, which would decrease splitting of

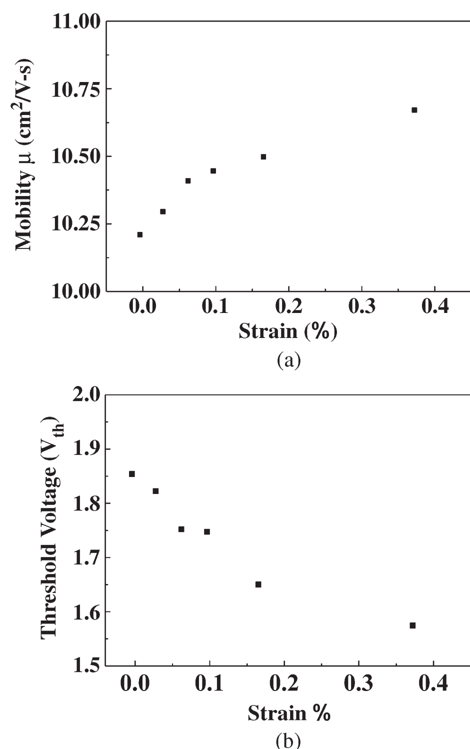

Fig. 10. (a) Linear mobility as a function of the mechanical strain. (b) Threshold voltage as a function of the mechanical strain for the flexible a-IGZO TFTs (under different bending radii).

energy levels and, in turn, results in a decrease in the band gap [28], [29]. With a smaller band gap, more electrons could be excited to the conduction band at the same thermal equilibrium condition [29]. Many previous studies of a-IGZO TFTs had shown that their threshold voltages and mobility had a strong correlation with carrier concentrations [7]. In general, higher carrier concentrations in a-IGZO would lead to lower threshold voltages and higher mobility values [30]. Such a picture appears to be consistent with higher mobility values and lower threshold voltages versus larger tensile strains. The nonlinear dependence of mobility and threshold voltage may be associated with band splitting that is nonlinear with increasing interatomic distances [28].

IV. Conclusion

In conclusion, we have successfully implemented flexible top-gate staggered a-IGZO TFTs on colorless and transparent PI-based nanocomposite substrates using fully lithographic, etching, and PECVD processes that are compatible with existing TFT mass fabrication technologies. The use of the selectively coated release layer between the nanocomposite PI film and the glass carrier ensured smooth debonding of the plastic substrate after TFT fabrication. The TFTs showed decent performances (with mobility $> 10\ \mathrm{cm}^2/\mathrm{V}\cdot\mathrm{s}$) either as fabricated or as debonded from the carrier glass. By bending the devices to different radii of curvature (from a flat state to an outward bending radius of 5 mm), influences of mechanical strains on the characteristics of the flexible a-IGZO TFTs were also investigated. In general, the mobility of the flexible a-IGZO TFTs increased with the tensile strain, whereas the threshold voltage decreased with the tensile strain. The variation of the mobility in a-IGZO TFTs versus the strain appeared smaller than those observed for a-Si TFTs.

References

[1] A. Nathan and R. Chalamala, "Flexible electronics technology, Part II: Materials and devices," *Proc. IEEE*, vol. 93, no. 8, pp. 1391–1393, Aug. 2005.

[2] C. Y. Lin, C. H. Tsai, H. T. Lin, L. C. Chang, Y. H. Yeh, Z. Pei, Y. R. Peng, and C. C. Wu, "High-frequency polymer diode rectifiers for flexible wireless power-transmission sheets," *Organ. Electron.*, vol. 12, no. 11, pp. 1777–1782, Nov. 2011.

[3] C. C. Wu, S. D. Theiuss, G. Gu, M. H. Lu, J. C. Strum, and S. Wagner, "Integration of organic LEDs and amorphous Si TFTs onto flexible and lightweight metal foil substrates," *IEEE Electron Device Lett.*, vol. 18, no. 12, pp. 609–612, Dec. 1997.

[4] J. H. Na, M. Kitamura, D. Lee, and Y. Arakawa, "High performance flexible pentacene thin-film transistors fabricated on titanium silicon oxide gate dielectrics," *Appl. Phys. Lett.*, vol. 90, no. 16, pp. 163 514-1–163 514-3, Apr. 2007.

[5] H. Gleskova, S. Wagner, and Z. Suo, "a-Si:H thin film transistors after very high strain," *J. Non-Cryst. Solids*, vol. 266–269, pp. 1320–1324, May 2000.

[6] H. Gleskova, P. I. Hsu, Z. Xi, J. C. Sturm, Z. Suo, and S. Wagner, "Field-effect mobility of amorphous silicon thin-film transistors under strain," *J. Non-Crystal. Solids*, vol. 338–340, pp. 732–735, Jun. 2004.

[7] K. Nomura, H. Ohta, A. Takagi, T. Kamiya, M. Hirano, and H. Hosono, "Room-temperature fabrication of transparent flexible thin-film transistors using amorphous oxide semiconductors," *Nature*, vol. 432, no. 7016, pp. 488–492, Nov. 2004.

[8] T. Kamiya, H. Hiramatsu, K. Nomura, and H. Hosono, "Device applications of transparent oxide semiconductors: Excitonic blue LED and transparent flexible TFT," *J. Electroceram.*, vol. 17, no. 2–4, pp. 267–275, Dec. 2006.

[9] A. Plichta, A. Weber, A. Habeck, and S. Glas, "Ultra-thin flexible glass substrates," in *Proc. Mater. Res. Soc. Symp.*, 2003, vol. 769, pp. H9.1–H9.10.

[10] I. C. Cheng, A. Kattamis, K. Long, J. C. Sturm, and S. Wagner, "Stress control for overlay registration in a-Si:H TFTs on flexible organic-polymer-foil substrates," *J. Soc. Inf. Display*, vol. 13, no. 7, pp. 563–568, Jul. 2005.

[11] W. A. MacDonald, "Engineered films for display technologies," *J. Mater. Chem.*, vol. 14, no. 1, pp. 4–10, 2004.

[12] W. B. Jackson, R. L. Hoffman, and G. S. Herman, "High-performance flexible zinc tin oxide field-effect transistors," *Appl. Phys. Lett.*, vol. 87, no. 19, pp. 193 503-1–193 503-3, Nov. 2005.

[13] J. S. Park, T. W. Kim, D. Stryakhilev, J. S. Lee, S. G. An, Y. S. Pyo, D. B. Lee, Y. G. Mo, D. U. Jin, and H. K. Chung, "Flexible full color organic light-emitting diode display on polyimide plastic substrate driven by amorphous indium gallium zinc oxide thin-film transistors," *Appl. Phys. Lett.*, vol. 95, no. 1, pp. 013503-1–013503-3, Jul. 2009.

[14] D. Zhao, D. A. Mourey, and T. N. Jackson, "Fast flexible plastic substrate ZnO circuits," *IEEE Electron Device Lett.*, vol. 31, no. 4, pp. 323–325, Apr. 2010.

[15] W. Lim, J. H. Jang, S. H. Kim, D. P. Norton, V. Craciun, S. J. Pearton, F. Ren, and H. Shen, "High performance indium gallium zinc oxide thin film transistors fabricated on polyethylene terephthalate substrates," *Appl. Phys. Lett.*, vol. 93, no. 8, pp. 082102-1–082102-3, Aug. 2008.

[16] K. H. Cherenack, N. S. Münzenrieder, and G. Tröster, "Impact of mechanical bending on ZnO and IGZO thin-film transistors," *IEEE Electron Device Lett.*, vol. 31, no. 11, pp. 1254–1256, Nov. 2010.

[17] M. C. Sung, H. N. Lee, C. N. Kim, S. K. Kang, D. Y. Kim, S. J. Kim, S. K. Kim, S. K. Kim, H. G. Kim, and S. T. Kim, "Novel backplane for AM-OLED device," in *Proc. IMID Symp.*, 2007, pp. 133–136.

[18] A. Dey, A. Indluru, S. M. Venugopal, D. R. Allee, and T. L. Alford, "Effect of mechanical and electromechanical stress on a-ZIO TFTs," *IEEE Electron Device Lett.*, vol. 31, no. 12, pp. 1416–1418, Dec. 2010.

[19] H. H. Hsieh, C. H. Wu, C. W. Chien, C. K. Chen, C. S. Yang, and C. C. Wu, "Influence of channel-deposition conditions and gate insulators on performance and stability of top-gate IGZO transparent thin-film transistors," *J. Soc. Inf. Display*, vol. 18, no. 10, pp. 796–801, Oct. 2010.

[20] K. Nomura, T. Kamiya, and H. Hosono, "Highly stable amorphous In–Ga–Zn–O thin-film transistors produced by eliminating deep subgap defects," *Appl. Phys. Lett.*, vol. 99, no. 5, pp. 053505-1–053505-3, Aug. 2011.

[21] H. S. Bae, J. H. Kwon, S. Chang, M. H. Chung, T. Y. Oh, J. H. Park, S. Y. Lee, J. J. Pak, and B. K. Ju, "The effect of annealing on amorphous indium gallium zinc oxide thin film transistors," *Thin Solid Films*, vol. 518, no. 22, pp. 6325–6329, Sep. 2010.

[22] J. M. Liu, T. M. Lee, C. H. Wen, and C. M. Leu, "High-performance organic–inorganic hybrid plastic substrate for flexible displays and electronics," *J. Soc. Inf. Display*, vol. 19, no. 1, pp. 63–69, Jan. 2011.

[23] C. W. Chien, C. H. Wu, Y. T. Tsai, Y. C. Kung, C. Y. Lin, P. C. Hsu, H. H. Hsieh, C. C. Wu, Y. H. Yeh, C. M. Leu, and T. M. Lee, "High-performance flexible a-IGZO TFTs adopting stacked electrodes and transparent polyimide-based nanocomposite substrates," *IEEE Trans. Electron Devices*, vol. 58, no. 5, pp. 1440–1446, May 2011.

[24] J. S. Kang, D. K. Schroder, and A. R. Alvarez, "Effective and field-effect mobilities in Si MOSFETs," *Solid-State Electron.*, vol. 32, no. 8, pp. 679–681, Aug. 1989.

[25] H. G. Lee, S. Y. Oh, and G. Fuller, "A simple and accurate method to measure the threshold voltage of an enhancement-mode MOSFET," *IEEE Trans. Electron Devices*, vol. ED-29, no. 2, pp. 346–348, Feb. 1982.

[26] M. Y. Han and J. H. Jou, "Determination of the mechanical properties of r.f.-magnetron-sputtered zinc oxide thin films on substrates," *Thin Solid Films*, vol. 260, no. 1, pp. 58–64, May 1995.

[27] M. Maeda and K. Ikeda, "Stress evaluation of radio-frequency-biased plasma-enhanced chemical vapor deposited silicon nitride films," *J. Appl. Phys.*, vol. 83, no. 7, pp. 3865–3870, Apr. 1998.

[28] A. Rockett, *Materials Science of Semiconductors*. New York: Springer-Verlag, 2007, ch. 5.

[29] K. Uchida, T. Krishnamohan, K. C. Saraswat, and Y. Nishi, "Physical mechanisms of electron mobility enhancement in uniaxial stressed MOSFETs and impact of uniaxial stress engineering in ballistic regime," in *IEDM Tech. Dig.*, 2005, pp. 129–132.

[30] J. H. Shin and D. K. Choi, "Effect of oxygen on the optical and the electrical properties of amorphous InGaZnO thin films prepared by RF magnetron sputtering," *J. Korean Phys. Soc.*, vol. 53, no. 4, pp. 2019–2023, Oct. 2008.

Chang-Yu Lin is currently working toward the Ph.D. degree at National Taiwan University, Taipei, Taiwan.

His research interests include organic electronics, oxide semiconductors thin-film transistor technologies, and flexible electronics and displays.

Chih-Wei Chien received the M.S. degree in electronics engineering from National Taiwan University, Taipei, Taiwan, in 2009.

He is currently a Research Associate with National Taiwan University.

Chung-Chih Wu received the Ph.D. degree in electrical engineering from Princeton University, Princeton, NJ, in 1997.

In 1998, he joined the faculty of National Taiwan University, Taipei, Taiwan, where he is currently a Full Professor.

Yung-Hui Yeh received the Ph.D. degree in electrical engineering from National Tsing Hua University, Hsinchu, Taiwan, in 1998.

In 1998, he joined the Industrial Technology Research Institute, Hsinchu, where he is currently a Deputy Director.

Chun-Cheng Cheng received the M.S. degree in electrical engineering from National Tsing Hua University, Hsinchu, Taiwan.

He is currently a Deputy Manager with the Industrial Technology Research Institute, Hsinchu.

Chih-Ming Lai received the Ph.D. degree in electrical engineering from National Tsing Hua University, Hsinchu, Taiwan.

He is currently a Deputy Manager with the Industrial Technology Research Institute, Hsinchu.

Ming-Jiue Yu is currently working toward the Ph.D. degree in electronics engineering at National Chiao Tung University, Hsinchu, Taiwan.

He is currently an Engineer with the Industrial Technology Research Institute, Hsinchu.

Chyi-Ming Leu received the Ph.D. degree in materials science engineering from National Chiao Tung University, Hsinchu, Taiwan, in 2003.

He is currently a Researcher with the Industrial Technology Research Institute, Hsinchu.

Tzong-Ming Lee received the Ph.D. degree in chemical engineering from National Tsing Hua University, Hsinchu, Taiwan, in 2005.

He is currently a Director with the Organic Electronic Materials Division, Industrial Technology Research Institute, Hsinchu.